Dynamic pathways to mediate reactions buried in thermal fluctuations

Shinnosuke Kawai [*] **and Tamiki Komatsuzaki** [*] [†]

[*]Molecule & Life Nonlinear Sciences Laboratory, Research Institute for Electronic Science, Hokkaido University, Kita 20 Nishi 10, Kita-ku, Sapporo 010-0020, Japan, and [†]Core Research for Evolutional Science and Technology (CREST), Japan Science and Technology Agency (JST), Kawaguchi, Saitama 332-0012, Japan

Submitted to Proceedings of the National Academy of Sciences of the United States of America

How a system can robustly undergo a reaction from one stable state to another in the presence of thermal fluctuations has been one of the most intriguing subjects in chemistry and biology. We present a theory which enables us to explore the mechanism of reaction selectivity and robust functions in complex systems persisting under thermal fluctuation. The theory constructs a nonlinear coordinate transformation so that the equation of motion for the new reaction coordinate is independent of the other non-reactive coordinates in the presence of thermal fluctuation. In this article we suppose reacting systems subject to thermal noise are described by a multi-dimensional Langevin equation with an arbitrary form of the potential of mean force. The reaction coordinate is composed not only of all the coordinates and velocities associated with the system (solute), but also of the random force exerted by the environment (solvent) with friction constants. The sign of the reaction coordinate at any instantaneous moment in the region of a saddle, in principle, determines the fate of the reaction, i.e., whether the reaction will proceed through to the products or go back to the reactants. The statistical properties of the reaction coordinate decoupled from all the other non-reactive coordinates in the presence of thermal noise are analyzed using the Müller-Brown potential with triple basins.

transition states in noisy environment | reaction selectivity | thermal fluctuation | robustness of functions

Chemical reactions are ubiquitous in nature, and can be regarded as prototypes of 'change of matter' [1]. The most common class of chemical reactions is a system moving on a single effective potential surface from one local minimum to another, through a saddle region. Chemists have long envisioned the existence of a dividing surface in the saddle region through which the system passes only once in going from one stable state to another. The surface is called the 'transition state (TS)' [2, 3, 4, 5, 6, 7, 8, 9]. The TS is supposed to lie transverse to a one-dimensional coordinate axis, called the 'reaction coordinate,' which describe the progress of the reaction. The concept of the TS has provided us with great insights for understanding not only the rate of chemical reactions but also, for example, ionization of a hydrogen atom in crossed electric and magnetic fields [10], isomerization of clusters [11], the escape of asteroids from Mars [12], and the folding/unfolding of proteins [13]. Despite these successful applications, the firm mathematical foundation for the existence of such a dividing surface was not fully established until recently. For instance, re-crossings over a "TS" which one locates naïvely (e.g. using harmonic approximations) have sometimes been observed, giving rise to a serious overestimation of the rate. However, following several developments in experiments [14] and theories [15, 16, 17, 18, 19] on characterizing the regularity in dynamics through saddles, recent developments of the phase space picture of TS has shown the existence of a rigorous dividing surface free from the problem of re-crossings even in a sea of chaos [20, ?, 10, 21, 22]. It was found that there exists a reaction coordinate in the phase space decoupled from the other nonreactive coordinates. This decoupling enables us to make an *a priori* prediction about the destination of the reaction at any instant (at least) in the region of a saddle. These recent developments of phase space TS theory are based on Hamiltonian systems which corresponds to "isolated molecules."

Most reactions in biology or chemical synthesis, however, occur in condensed phase. The most characteristic difference from the isolated system is that the system (e.g., solute) is subject to external forces exerted by the surrounding environment (e.g., solvents). Even for a fixed initial condition of all the variables in the system, the final destination is not necessarily unique but has a certain probability distribution because one cannot control the external force due to its stochastic nature. In the pioneering studies by Kramers [23] (and later by Grote and Hynes [24]), condensed phase reactions are described in terms of (generalized) Langevin equations in which the system moves along a one-dimensional coordinate (in the configuration space) on the potential of mean force under the influence of friction (friction kernel) and the random force exerted by the environment. The system-bath Hamiltonian approach can formally bridge the descriptions of *any* Hamiltonian system and the generalized Langevin formulation [25, 26, 27] projected onto an arbitrarily chosen coordinate. The question of the description of dynamical systems in the presence of thermal fluctuation is one of the most intriguing subjects in nonequilibrium statistical mechanics [28, 29]. In addition, there remains the fundamental question of what reaction coordinate a system *actually* follows under the disturbance of thermal fluctuation. In this article we use the term 'reaction coordinate' to mean a single coordinate that can describe the progress of the reaction and show the destination of the reaction at any instant without referring to the other coordinates. The existence of the reaction coordinate for multiple nonlinearly coupled modes in thermally fluctuating environments, as well as the method for extracting it, is not a trivial problem.

To deal with the problem of nonlinearity of multimode reacting systems in condensed phase, the variational transition state theory (VTST) has been applied with explicit harmonic bath modes [30, 31, 32]. VTST has provided excellent physical insights about the location of the dividing surface as well as improved expressions for rate constants. In practice, however, VTST needs a certain small number of selected variables to parameterize the dividing surface (usually position coordinate(s) of the system (e.g., solute)), and it is very hard to derive the reaction coordinate to enable us to robustly predict the destination of reaction. This is because the reaction

Reserved for Publication Footnotes

coordinate must be, in principle, a nonlinear function of all the position coordinates and velocities of the reacting system and all the effects exerted by the surroundings. In addition to the studies applying VTST, a few studies have been performed to locate a boundary between the mainly reactive region and the mainly nonreactive region in the position-velocity space of dissipative reaction systems. Here the words "mainly (non-)reactive" mean the reaction probability is more (less) than one half [33, 34, 35]. However, these studies have so far been performed only in very limited situations. The generalization to nonlinear many degrees-of-freedom (dof) systems (the most typical situation for realistic systems) has been an open, unresolved problem.

In this article, we present a theory to single out a new reaction coordinate decoupled from the other non-reactive coordinates in the presence of thermal fluctuations. Here we assume that reacting systems are described by the framework of multi-dimensional (underdamped) Langevin equation. The term "underdamped" means that the second time derivative of the position $\boldsymbol{q}$ is included in the equation of motion, which is distinguished from the "overdamped" case of $\ddot{\boldsymbol{q}} = 0$ where equilibration in the velocity ($\dot{\boldsymbol{q}}$) space is supposed to be attained much more quickly than in the position ($\boldsymbol{q}$) space. We show that the sign of the new coordinate at any instantaneous moment in the saddle region *in principle* determines the fate of the reaction: that is whether the system reaction will go forward to the products or go back to the reactants. By assuming the statistical properties of the random force, one can know *a priori* a well-defined boundary of the reaction which separates the full position-velocity space (spanned by the position $\boldsymbol{q}$ and the velocity $\dot{\boldsymbol{q}}$) in the saddle region into mainly-reactive and mainly-nonreactive regions even under thermal fluctuation. In addition to obtaining the reaction boundary, the introduction of the new coordinate provides detailed insights into the flows of trajectories in the position-velocity space. The analytical expression for the new reaction coordinate in terms of $(\boldsymbol{q}, \dot{\boldsymbol{q}})$ of the system and the random force $\boldsymbol{\xi}(t)$ from the solvent enables us to obtain physical insights about the pathway to mediate the reaction.

The main interest of this article is the question of the general existence of a reaction coordinate in the position-velocity space by which one can predict the destination of a reaction in a thermally fluctuating environment. For simplicity, our theory will be presented in the framework of the underdamped multidimensional Langevin formulation. The extension to the generalized Langevin formulation will be presented in a separate paper.

Results and discussions

Fig. 1 shows two examples of trajectories with the contours of the potential of mean force. The green line shows a reactive trajectory that starts on one side of the "barrier," which is here defined naïvely as $q_1 = 0$, passes over it and goes to the other side. The red line is a non-reactive trajectory that crosses the "barrier" but is reflected back into its original region. The trajectories follow an n-dimensional Langevin equation:

$$\ddot{\boldsymbol{q}} = -\frac{\partial U}{\partial \boldsymbol{q}} - \gamma \dot{\boldsymbol{q}} + \boldsymbol{\xi}(t), \qquad [1]$$

where $\boldsymbol{q} = (q_1, \ldots, q_n)^{\mathrm{T}}$ is the position coordinates of the system (solute), U the potential of the mean force, γ the friction constant, and $\boldsymbol{\xi}(t)$ describes the random force from the solvent. As an illustrative example, we use the Müller-Brown potential [36] [See Supporting Information (SI)]. In this example, the dimension n is two, but our theory presented in this paper is applicable to systems of any dimension. The trajectory calculation is performed [37] with the random force sampled according to the fluctuation-dissipation theorem

$$\langle \boldsymbol{\xi}(t) \boldsymbol{\xi}(0)^{\mathrm{T}} \rangle = 2 k_{\mathrm{B}} T \gamma \delta(t), \qquad [2]$$

where $\boldsymbol{\xi}(0)^{\mathrm{T}}$ is the transpose of the vector $\boldsymbol{\xi}(0)$, T the temperature and k_{B} Boltzmann constant. The force from the potential U can be expanded in a Taylor series

$$-\frac{\partial U}{\partial q_j} = -k_j q_j + \sum\nolimits_{|\boldsymbol{m}|\geq 2} \alpha_{j,\boldsymbol{m}} q_1^{m_1} \cdots q_n^{m_n}, \qquad [3]$$

with the expansion coefficients k_j and $\alpha_{j,\boldsymbol{m}}$ for the linear and the nonlinear parts, respectively. Here, $|\boldsymbol{m}| = \sum_j m_j$ and $\sum_{|\boldsymbol{m}|\geq 2}$ sums over combinations of m_j satisfying $|\boldsymbol{m}| \geq 2$.

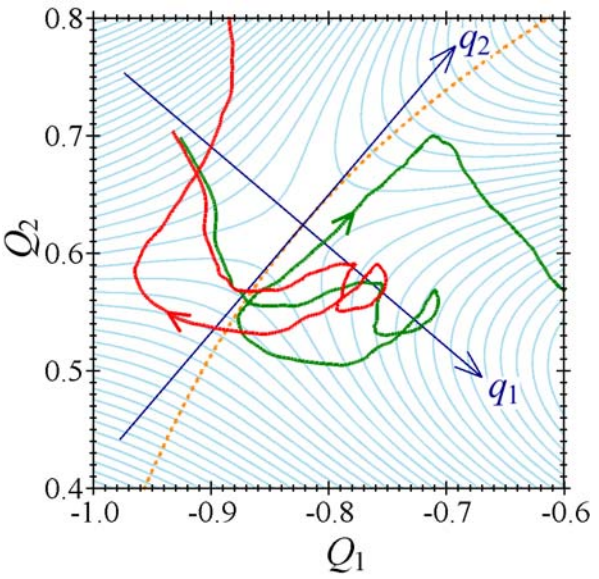

Fig. 1. Examples of trajectories with the effects of friction and random force, shown superimposed with contours of the Müller-Brown potential energy surface [36]. The horizontal and vertical axes are the position coordinates originally used to describe the Müller-Brown surface. The configuration space normal mode coordinates (q_1, q_2) are also shown. The friction is chosen to be $\gamma = 30$, which is comparable with the harmonic frequencies at the saddle point (27 for reactive and 22 for non-reactive). The temperature is below the barrier height relative to the minima (See also SI for the details). A reactive trajectory is shown by the green line, and a non-reactive trajectory is shown in red. The coordinate q_1 corresponds to the reactive direction, and q_2 corresponds to the non-reactive (vibrational) mode. The ridge of the potential is shown by the orange dotted line.

In Fig. 3(a), the trajectories are plotted in position (q_1) and velocity ($\dot{q}_1$) along the reactive direction. The velocity fluctuates more significantly than the position, due to the random force. The direction of q_1 in the configuration space is shown in Fig. 1. In Fig. 3(a), we also show the normal mode coordinates (u_1, u_2) in the position-velocity space that diagonalize the linear part

$$\frac{d}{dt}\begin{pmatrix}\boldsymbol{q}\\ \dot{\boldsymbol{q}}\end{pmatrix} = \begin{pmatrix}\boldsymbol{0} & \boldsymbol{1}\\ \boldsymbol{K} & -\boldsymbol{\Gamma}\end{pmatrix}\begin{pmatrix}\boldsymbol{q}\\ \dot{\boldsymbol{q}}\end{pmatrix}, \qquad [4]$$

where $\boldsymbol{1}$ is $n \times n$ unit matrix, $\boldsymbol{\Gamma}$ is equal to $\gamma \boldsymbol{1}$, and $\boldsymbol{K}$ is the Hessian matrix of U at $\boldsymbol{q} = \boldsymbol{0}$. The normal mode coordinate

$\boldsymbol{u} = (u_1, u_2, \ldots, u_{2n})^{\mathrm{T}}$ is obtained by diagonalizing the matrix

$$\boldsymbol{V}^{-1}\begin{pmatrix}\boldsymbol{0} & \boldsymbol{1}\\ \boldsymbol{K} & -\boldsymbol{\Gamma}\end{pmatrix}\boldsymbol{V} = \mathrm{diag}(\lambda_1, \cdots, \lambda_{2n}),$$
$$\begin{pmatrix}\boldsymbol{q}\\ \dot{\boldsymbol{q}}\end{pmatrix} = \boldsymbol{V}\,\boldsymbol{u} \qquad [5]$$

The numbering of the eigenvalues is such that $\lambda_1 > 0$ corresponds to the unstable motion sliding down the barrier.

After the diagonalization, the equation of motion becomes

$$\frac{d}{dt}u_j = \lambda_j u_j + \tilde{\xi}_j(t) + \sum\nolimits_{|\boldsymbol{m}|\geq 2}\beta_{j,\boldsymbol{m}}u_1^{m_1}u_2^{m_2}\cdots u_{2n}^{m_{2n}}, \qquad [6]$$

where $\tilde{\boldsymbol{\xi}}(t) = \boldsymbol{V}\begin{pmatrix}\boldsymbol{0}\\ \boldsymbol{\xi}(t)\end{pmatrix}$, and the coefficients $\beta_{j,\boldsymbol{m}}$ are obtained by substituting Eq. (5) into the nonlinear terms in Eq. (3). The surface defined by $u_1 = 0$ would perform the role of the boundary between reactive and non-reactive trajectories if there were no random force or nonlinearities. In reality, however, trajectories cross the $u_1 = 0$ axis many times due to the random force and nonlinear couplings as seen in Fig. 3(a).

Recent studies [38, 39, 40, 41] introduced relative coordinates, which we call x_j here, by

$$u_j = S[\lambda_j, \tilde{\xi}_j](t) + x_j \qquad [7]$$

where we have introduced a notation S as in Refs. [41, 42]:

$$S[\lambda_j, \tilde{\xi}_j](t) = \begin{cases} \int_{-\infty}^{0}\exp(-\lambda_j\tau)\tilde{\xi}_j(t+\tau)d\tau & (\mathrm{Re}\lambda_j < 0)\\ -\int_{0}^{+\infty}\exp(-\lambda_j\tau)\tilde{\xi}_j(t+\tau)d\tau & (\mathrm{Re}\lambda_j > 0)\end{cases} \qquad [8]$$

Then the equation of motion for $\boldsymbol{x}$ is given by

$$\frac{d}{dt}x_j = \lambda_j x_j + \sum\nolimits_{|\boldsymbol{m}|\geq 0} f_{j,\boldsymbol{m}}(t)x_1^{m_1}x_2^{m_2}\cdots x_{2n}^{m_{2n}}, \qquad [9]$$

where the coefficients $f_{j,\boldsymbol{m}}(t)$ are obtained from the nonlinear terms in Eq. (6). The expansion coefficients $f_{j,\boldsymbol{m}}(t)$ are now time-dependent due to the time-dependent shift [Eq. (7)]. If there were no nonlinear terms in the potential U, the equation of motion in x_1 would not depend on the random force. Then the solution would be $x_1(t) = x_1(t_0)\exp[\lambda_1(t-t_0)]$ where t_0 is a certain instant of time. Since $\lim_{t\to+\infty}\exp[\lambda_1(t-t_0)] = \infty$, the system would move away from the barrier region as t increases, with the direction [the sign of $x_1(t)$] determined solely by the sign of $x_1(t_0)$. Fig. 3(b) shows plots of the two trajectories in the relative coordinates (x_1, x_2). The trajectories have become much smoother than the corresponding plots in Fig. 3(a). This implies that the shift of coordinates [38, 39, 40, 41] incorporates the effect of the random force to some extent. However, the non-reactive trajectory starts at $x_1 > 0$, crosses the line $x_1 = 0$, and finally returns to the left side of the figure. Therefore this line still does not function as the boundary of reaction when significant nonlinearities exist in the potential U.

A hidden coordinate for reactions under thermal fluctuation: Here we introduce a nonlinear transformation from $\boldsymbol{x}$ to $\boldsymbol{y}$ so that the equation of motion for y_1 contains no coupling with the other coordinates, that is,

$$\frac{d}{dt}y_1 \approx \{\lambda_1 + c_1(t)\}\,y_1, \qquad [10]$$

with a time-dependent coefficient $c_1(t)$. The procedure is given in Materials and Methods and SI. Eq. (10) tells us that, if $c_1(t)$ does not exceed λ_1 in magnitude, the system moves away from the barrier region, with the direction given by the sign of $y_1(t_0)$ at any instant of time t_0, irrespective of $y_2, y_3, \ldots$. Fig. 3(c) plots the two trajectories in the normal form coordinates (y_1, y_2). It is clearly seen that $y_1 = 0$ separates correctly the reactive and the non-reactive trajectories. The transformation from the original coordinates $(\boldsymbol{q}, \dot{\boldsymbol{q}})$ (through $\boldsymbol{u}$ and $\boldsymbol{x}$) to $\boldsymbol{y}$ can be expressed in the form of a polynomial expansion

$$\begin{aligned} y_1 =& a_1 q_1 + a_2\dot{q}_1 - S[\lambda_1, \tilde{\xi}_1](t) + F_0[\boldsymbol{\lambda}, \boldsymbol{\xi}](t)\\ &+ \sum\nolimits_{|\boldsymbol{m}|\geq 2} w_{\boldsymbol{m}}{q_1}^{m_1}\cdots{q_n}^{m_n}{\dot{q}_1}^{m_{n+1}}\cdots{\dot{q}_n}^{m_{2n}}\\ &+ \sum_{|\boldsymbol{m}|\geq 1} F_{\boldsymbol{m}}[\boldsymbol{\lambda}, \boldsymbol{\xi}](t){q_1}^{m_1}\cdots{q_n}^{m_n}{\dot{q}_1}^{m_{n+1}}\cdots{\dot{q}_n}^{m_{2n}} \end{aligned} \qquad [11]$$

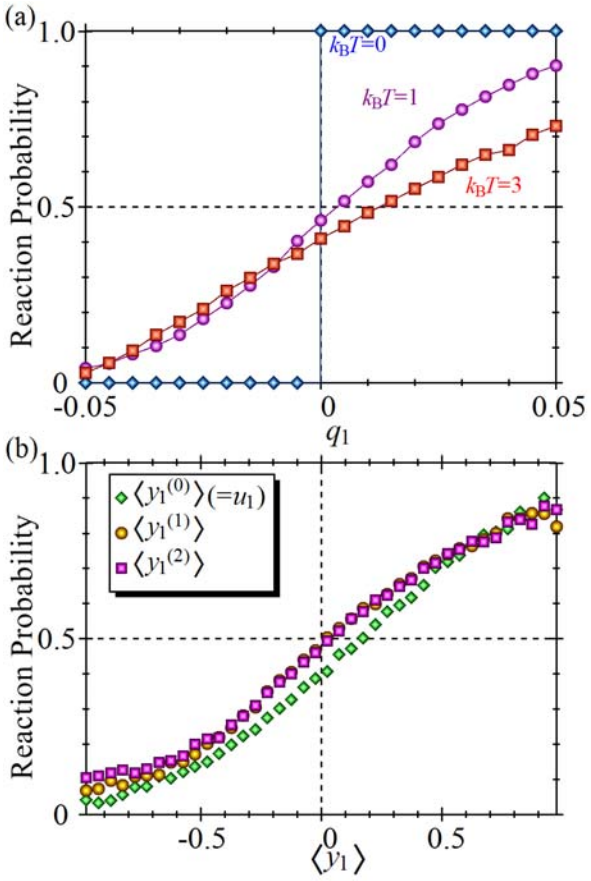

Fig. 2. Reaction probabilities as functions of (a) the normal mode reaction coordinate q_1, and (b) the normal form reaction coordinate $\langle y_1\rangle$ averaged over the random forces. In (a), $k_BT = 0$ (diamond), 1 (circle), and 3 (square). The reaction probability for a surface of $q_1 = \alpha$ is given by $P_{\mathrm{reaction}}(q_1 = \alpha) = \int d\boldsymbol{q}d\dot{\boldsymbol{q}}\delta(q_1 - \alpha)P(\boldsymbol{q}, \dot{\boldsymbol{q}})\exp(-E(\boldsymbol{q}, \dot{\boldsymbol{q}})/k_BT) / \int d\boldsymbol{q}d\dot{\boldsymbol{q}}\delta(q_1 - \alpha)\exp(-E(\boldsymbol{q}, \dot{\boldsymbol{q}})/k_BT)$. Here we took each surface of constant q_1 on which all the other $(\boldsymbol{q}, \dot{\boldsymbol{q}})$ are sampled according to the Boltzmann distribution. Then the trajectory calculation was performed starting from these initial conditions with different instances of random forces $\boldsymbol{\xi}$ satisfying Eq. (2) with the same k_BT. $P(\boldsymbol{q}, \dot{\boldsymbol{q}})$ and $E(\boldsymbol{q}, \dot{\boldsymbol{q}})$, respectively, denote the reaction probability for a given initial condition $(\boldsymbol{q}, \dot{\boldsymbol{q}})$ and a sum of the kinetic and the potential energies $E(\boldsymbol{q}, \dot{\boldsymbol{q}}) = (\dot{q}_1^2 + \dot{q}_2^2)/2 + V(q_1, q_2)$. In (b), plots for zero-th, first, and second order perturbation are shown at $k_BT = 3$ in diamond, circle, and square, respectively. The reaction probability for a surface of $\langle y_1\rangle = \beta$ is given by $P_{\mathrm{reaction}}(\langle y_1\rangle = \beta; q_1 = 0) = \int d\boldsymbol{q}d\dot{\boldsymbol{q}}\delta(q_1)\delta(\langle y_1\rangle - \beta)\,P(\boldsymbol{q}, \dot{\boldsymbol{q}})\exp(-E(\boldsymbol{q}, \dot{\boldsymbol{q}})/k_BT) / \int d\boldsymbol{q}d\dot{\boldsymbol{q}}\delta(q_1)\delta(\langle y_1\rangle - \beta)\exp(-E(\boldsymbol{q}, \dot{\boldsymbol{q}})/k_BT)$. Here $\langle y_1\rangle$ is calculated as a function of $(\boldsymbol{q}, \dot{\boldsymbol{q}})$ by Eq (12). We took the same simulation data for $q_1 = 0$ as used in the numerical simulation of (a).

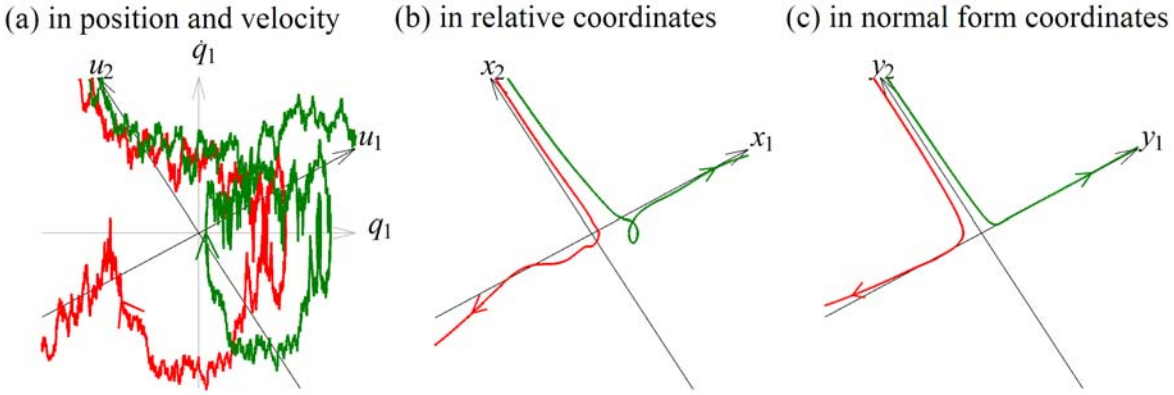

Fig. 3. Examples of trajectories (same as Fig. 1) plotted in three sets of coordinates. (a) Trajectories plotted in the position-velocity space. The normal mode coordinates (u_1, u_2) in the position-velocity space, which diagonalize the linearized equation of motion, are also shown. (b) Trajectories plotted in relative coordinates (x_1, x_2), obtained by subtracting the reference trajectory from (u_1, u_2). The trajectories have become smooth but cross the line $x_1 = 0$. (c) Trajectories plotted in normal form coordinates (y_1, y_2), obtained through a nonlinear transformation from (x_1, x_2). The coordinates are obtained by second order perturbation to normalize the equation of motion for both y_1 and y_2. The space defined by $y_1 = 0$ now functions as a boundary that separates the reactive and the non-reactive trajectories.

Eq. (11) enables us to interpret the reason why reactions take place in terms of various effects. The first two terms come from the linear approximation where coefficients a_1 and a_2 depend solely on the harmonic part of the potential of mean force and the friction constant. The term $S[\lambda_1, \tilde{\xi}_1](t)$ is interpreted as the motion arising from direct excitation by the "kick" from the solvent along the reactive direction. The nonlinear terms with coefficients $w_{\boldsymbol{m}}$ describe the driving force of the reaction arising from the nonlinearity inherent to the system (solute) because they appear even in the absence of the random forces. The term $F_0[\boldsymbol{\lambda}, \boldsymbol{\xi}](t)$ is a nonlinear functional of the random force $\xi_i(t)$ along all the directions $(i = 1, \ldots, n)$. This term arises only when there exist both the solvent force $\boldsymbol{\xi}(t)$ and the nonlinearity in the potential $\boldsymbol{U}$. For example, the vibration of the non-reactive mode is excited by the kick from the solvent (e.g., by ξ_2), which then affects the reaction through the nonlinear coupling between the reactive and the non-reactive modes. The terms with the time-dependent coefficient $F_{\boldsymbol{m}}[\boldsymbol{\lambda}, \boldsymbol{\xi}](t)$ describe the change of the magnitude of coupling depending on the random force $\boldsymbol{\xi}(t)$: the direct excitation by the solvent disturbs the position of the system in the configuration space, and the strength of nonlinear coupling can depend on the position.

The transformation to y_1 depends on each instance of the stochastic forces $\boldsymbol{\xi}(t)$. Theoretically, if one knew the time series of $\boldsymbol{\xi}(t)$ for all t in advance, one could precisely predict the fate of the reaction within the order of perturbation. Eq. (8) also requires all the future values of $\tilde{\xi}_j$ for $\mathrm{Re}\lambda_1 > 0$, and all the past values for $\mathrm{Re}\lambda_j < 0$. In realistic situations, the system cannot "know" the time evolution of $\boldsymbol{\xi}(t)$ for each instance in advance. What one may assume is the characteristic properties of random forces as 'an ensemble' rather than a single instance. To look into the question of how the dynamical structure persists under thermal fluctuation, we consider the ensemble average of y_1 with respect to thermal noise:

$$\begin{aligned}\langle y_1 \rangle =& a_1 q_1 + a_2 \dot{q}_1 + \bar{F}_0(k_{\mathrm{B}}T) \\ &+ \sum\nolimits_{|\boldsymbol{m}|\geq 2} w_{\boldsymbol{m}} {q_1}^{m_1} \cdots {q_n}^{m_n} {\dot{q}_1}^{m_{n+1}} \cdots {\dot{q}_n}^{m_{2n}} \\ &+ \sum\nolimits_{|\boldsymbol{m}|\geq 1} \bar{F}_{\boldsymbol{m}}(k_{\mathrm{B}}T) {q_1}^{m_1} \cdots {q_n}^{m_n} {\dot{q}_1}^{m_{n+1}} \cdots {\dot{q}_n}^{m_{2n}} \quad [12]\end{aligned}$$

where the time-independent coefficients $\bar{F}_0(k_{\mathrm{B}}T)$ and $\bar{F}_{\boldsymbol{m}}(k_{\mathrm{B}}T)$ are the averages of the corresponding terms in Eq. (11) and are functions of temperature through Eq. (2). The direct solvent effect $S[\lambda_1, \tilde{\xi}_1](t)$ in Eq. (11) has the same probability for both signs in y_1 for the ensemble of $\tilde{\xi}_1(t)$ and hence vanishes in Eq. (12). Its effect is only in the fluctuation of y_1 around the average. This term does not provide any information concerning the persistence of the dynamical structure of the system against thermal noise. The terms with F_0 and $F_{\boldsymbol{m}}$ describing the 'nonlinear cooperation' between the system and the environment and those with $w_{\boldsymbol{m}}$ arising from the nonlinearity intrinsic to the system are crucial for understanding the mechanism of the robustness under thermal fluctuation, which cannot be obtained within the linear approximation [38, 39, 40, 41].

"Surfing" through a saddle with significant nonlinearity: Fig. 2(a) shows the numerical results of reaction probabilities P_{reaction}, for three different temperature

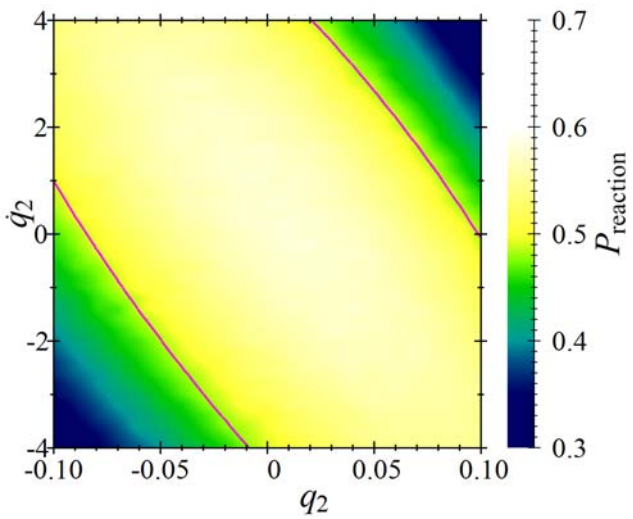

Fig. 4. Reaction probability as a function of non-reactive mode coordinates $(q_2, \dot{q}_2)$ at $t = 0$ obtained from numerical simulations with $k_{\mathrm{B}}T = 1$. Purple line is given by the equation $\langle y_1 \rangle = 0$ calculated using second order normal form perturbation theory. The initial conditions for the reactive mode were chosen as $(q_1, \dot{q}_1)|_{t=0} = (0.008, 0)$ because this value can be regarded as the most representative situation exhibiting the non-reactive mode dependence of the reaction probability.

$k_BT = 0, 1, 3$, as functions of q_1 (i.e., the reactive normal mode in the coordinate space). They are obtained for one saddle on the Müller-Brown potential where the nonlinearity of the potential is relatively high (The corresponding results at the other saddle are presented in SI). The barrier heights are about 41 and 107 between the saddle and the two minima which it links. Here $k_BT = 0$ corresponds to the situation where there is no random force [Eq. (2)] and no initial excitation along the non-reactive mode. Therefore $P_{\rm reaction}$ is either 0 or 1. The positive side ($q_1 > 0$) is reactive and the negative side ($q_1 < 0$) is non-reactive. Therefore the halfway point ($P_{\rm reaction} = 1/2$) at $q_1 = 0$ can be regarded as the boundary between the reactive and the non-reactive initial conditions at zero temperature. As the temperature increases, $P_{\rm reaction}$ takes intermediate values between 0 and 1. This results in broadening of the plot of $P_{\rm reaction}$ in Fig. 2(a) compared to the step-like behaviour at $k_BT = 0$. The major origin of this broadening was found to be the fluctuation of the direct solvent effect $S[\lambda_1, \tilde{\xi}_1](t)$ in Eq. (11) for the ensemble of $\tilde{\xi}_1(t)$. Moreover, the boundary of the reaction ($P_{\rm reaction} = 1/2$) is significantly shifted to the positive-q_1 direction. It indicates that the normal mode picture q_1 cannot provide us insights about the fate of the reaction.

In turn, Fig. 2(b) shows $P_{\rm reaction}$ at $k_BT = 3$ as a function of the normal form reaction coordinate $\langle y_1 \rangle$, which is $y_1(\boldsymbol{q}, \dot{\boldsymbol{q}}; \boldsymbol{\lambda}, \boldsymbol{\xi})$ averaged over all the different realizations of random force $\boldsymbol{\xi}(t)$ with the Boltzmann distribution for $(\boldsymbol{q}, \dot{\boldsymbol{q}})$ at $q_1 = 0$. We have confirmed a similar behavior for other values of q_1 (See SI). In the evaluation of $\langle y_1 \rangle$, the perturbation series of the normal form calculation was truncated at the zero-th, first, and second order, respectively, for the three different symbols in Fig. 2(b) (The analytical expression for y_1 and $\langle y_1 \rangle$ in terms of $\boldsymbol{q}$ and $\dot{\boldsymbol{q}}$ up to the second order are given in SI). One can see that, as the order of the perturbation increases, the halfway point $P_{\rm reaction} = 1/2$ comes closer to the origin $\langle y_1 \rangle = 0$. This shows that the normal form theory correctly gives the location of the boundary of reaction between the 'mainly-reactive' region and the 'mainly-nonreactive' region even in the presence of thermal fluctuation.

The dynamical nature of the present theory allows an investigation of the reaction probability for each initial condition before taking the average over the initial conditions for the non-reactive modes. Figure 4 demonstrates $P_{\rm reaction}$ as a function of non-reactive mode coordinate $(q_2, \dot{q}_2)|_{t=0}$ by the gradation of color with an initial condition for the reactive mode fixed. Since we scan only the non-reactive coordinates, the zero-th order linear approximation [38, 39, 40, 41], which neglects any coupling between the reactive and the non-reactive modes, would predict a uniform $P_{\rm reaction}$ irrespective of which and how non-reactive modes are excited. In reality, however, there exists non-uniformity in $P_{\rm reaction}$ as a function of the non-reactive mode $(q_2, \dot{q}_2)|_{t=0}$ in Fig. 4. Although the change of reaction probability is not a sudden jump from 0 to 1 due to the stochastic nature of the external force, we can still find a distinction between 'mainly reactive' region (that with lighter colors), and 'mainly non-reactive' one (with darker colors).

The purple line in Fig. 4 is obtained by the equation $\langle y_1 \rangle = 0$ in the second order normal form calculation. One can see that this line manifestly separates the mainly reactive region from the mainly non-reactive one. The most striking consequence in our theory is that one can *analytically* calculate the natural boundary of reaction *in principle* without performing trajectory simulations when one can assume the statistical property of random force $\boldsymbol{\xi}(t)$. This implies that one can predict *a priori* which initial conditions $(\boldsymbol{q}, \dot{\boldsymbol{q}})|_{t=0}$ of the system in the saddle region carry the system into the products with high probabilities, even when there is thermal noise.

The reaction mechanism under thermal fluctuation: Our theory is also capable of providing a firm interpretation of the mechanism for reaction under thermal fluctuation by looking at expression of y_1 or $\langle y_1 \rangle$ in terms of the original coordinates $(\boldsymbol{q}, \dot{\boldsymbol{q}})$. For example, what is the primary driving force making the reaction boundary $P_{\rm reaction} = 1/2$ migrate outward to the region of $q_1 > 0$ when temperature T increases from zero? Quantitative inspection of the terms in Eqs. (11) and (12) (see the details in SI) has shown that the main contribution arises from the combined effect in which the non-reactive mode is first excited by the "kick" from the environment and then the excitation of the non-reactive mode makes the reaction boundary shift toward the positive direction in q_1: the ridge of the potential surface around the saddle (Fig. 1) has a curved shape toward the positive direction of q_1. Hence, as the non-reactive mode is excited vibrationally, the effective position of the barrier along the reactive direction shifts toward the positive side.

The theory presented here is based on perturbation theory, and therefore its validity relies on the convergence of the expansion. The breakdown of the perturbation means disappearance of the dynamical structure separating the reactive and the non-reactive trajectories, and therefore is likely to lead to a purely stochastic reaction. The present theory is expected to provide a dynamical foundation for the appearance of purely stochastic processes in reactions in thermally fluctuating environments.

Outlook

In contrast to isolated systems in gas phase, reacting systems in solution are inherently subject to disturbance by the surrounding solvent molecules. For example, when one prepares molecules in specific vibrational states experimentally by laser excitation [43], the strong perturbation by the environment may cause dephasing of the states very quickly compared with the time scale of reaction. Nevertheless, Fig. 4 shows that the reaction boundary (or P_{fold} in the protein folding community) can survive even in a fluctuating environment, with the location predicted analytically by our present framework. We believe this to be a significant step toward controlling a reaction by selecting initial conditions that lead to the reaction with high probability, although several things remain to be considered such as quantum effects [44, 45]. The framework presented in this article may also contribute to the fundamental understanding of why biological (nonlinear) systems can robustly perform their functions even though the chemical energy of ATP hydrolysis is of comparable order to k_BT, the energy of stochastic, thermal fluctuations.

Materials and Methods

We extend the non-Hamiltonian normal form theory in Ref. [46] to time-dependent systems. The calculation proceeds in a similar way to Lie canonical perturbation theory [47, **?**] (a classical analog of Van Vleck perturbation theory). The equation of motion in $\boldsymbol{x}$ [Eq. (9)] is cast into

$$\frac{d}{dt} y_j = \lambda_j y_j + c_j(\boldsymbol{y}, t), \qquad \textbf{[13]}$$

by the transformation $x_j = y_j + w_j(\boldsymbol{y}, t)$. Introducing polynomial expansions for two unknown functions (c_j and w_j) as

$$c_j(\boldsymbol{y}, t) = \sum\nolimits_{\boldsymbol{m}} c_{j,\boldsymbol{m}}(t) {y_1}^{m_1} \cdots {y_{2n}}^{m_{2n}},$$
$$w_j(\boldsymbol{y}, t) = \sum\nolimits_{\boldsymbol{m}} w_{j,\boldsymbol{m}}(t) {y_1}^{m_1} \cdots {y_{2n}}^{m_{2n}} \qquad \textbf{[14]}$$

The coefficients $w_{j,\boldsymbol{m}}(t)$ are determined so as to diminish $c_{j,\boldsymbol{m}}(t)$ order by order: Substituting these unknown functions into Eq. (9), we obtain

$$\left(\langle\boldsymbol{\lambda},\boldsymbol{m}\rangle-\lambda_j+\frac{d}{dt}\right)w_{j,\boldsymbol{m}}(t)=g_{j,\boldsymbol{m}}(t)-c_{j,\boldsymbol{m}}(t), \qquad [15]$$

Where $\langle\boldsymbol{\lambda},\boldsymbol{m}\rangle=\sum_{k=1}^{2n}\lambda_k m_k$ and $g_{j,\boldsymbol{m}}(t)$ are the coefficients of the polynomial expansion of $g_j(\boldsymbol{y},t)\stackrel{\text{def}}{=}f_j(\boldsymbol{y}+\boldsymbol{w},t)-\sum_{i=1}^{2n}c_i(\boldsymbol{y},t)\frac{\partial w_j(\boldsymbol{y},t)}{\partial y_i}$. As is shown in SI, in the process of determining $c_{j,\boldsymbol{m}}(t)$ and $w_{j,\boldsymbol{m}}(t)$ perturbationally order by order, $g_{j,\boldsymbol{m}}(t)$ is known from the results of the lower orders. There thus exist two unknown quantities $c_{j,\boldsymbol{m}}(t)$ and $w_{j,\boldsymbol{m}}(t)$ with the known $g_{j,\boldsymbol{m}}(t)$ at each order. One can then determine either of the two unknown quantities as one wishes. To simplify the equation of motion for the new variables y_1, one can eliminate $c_{1,\boldsymbol{m}}(t)$ order by order by setting

$$w_{1,\boldsymbol{m}}(t)=S\left[\lambda_1-\langle\boldsymbol{\lambda},\boldsymbol{m}\rangle,g_{1,\boldsymbol{m}}\right](t), \qquad [16]$$

using the S-symbol as in Eqs. (7) and (8) [41, 42]. For $m_1=1,m_2=\cdots=m_{2n}=0$, we have $\lambda_1-\langle\boldsymbol{\lambda},\boldsymbol{m}\rangle=0$, for which case the S-symbol cannot be defined. This makes it necessary to incorporate a term $c_{1,\boldsymbol{m}}(t)$ in Eq. (15), where $m_1=1,m_2=\cdots=m_{2n}=0$. This is the reason why a time-dependent coefficient for y_1 remains in Eq. (10). The solution of Eq. (10) is given by

$$y_1(t)=y_1(t_0)\exp\left[\int_{t_0}^{t}\left(\lambda_1+c_1(t')\right)dt'\right], \qquad [17]$$

where t_0 is a certain instant of time (the initial condition). The exponent in Eq. (17) goes to infinity as $t\to+\infty$ if the long-time average of the perturbative term $c_1(t)$ is less than λ_1. Since λ_1 is $O(1)$ and $c_1(t)$ is $O(\varepsilon)$ with a small parameter ε in the perturbation calculation, this inequality can usually be expected to hold. As long as this condition is fulfilled, the sign of y_1 at time t_0 can predict the destination of the reaction **a priori** before the system reaches either the reactant or the product region. More detailed description is given in SI.

ACKNOWLEDGMENTS. We thank Profs. Turgay Uzer and Thomas Bartsch for letting us know contents of their research in advance, and Prof. Mikito Toda for stimulating discussions. This work has been supported by Research Fellowships of the Japan Society for the Promotion of Science for Young Scientists (to SK) and by JSPS, JST/CREST, Priority Area 'Molecular Theory for Real Systems' (to TK).

1. Levine R. D. (2005) Molecular Reaction Dynamics. (Cambridge University Press, Cambridge).
2. Eyring H. (1935) The activated complex in chemical reactions J. Chem. Phys. 3:107–115.
3. Wigner E. (1937) Calculation of the rate of elementary association reactions J. Chem. Phys. 5:720–725.
4. Evans M. G, Polanyi M. (1935) Some applications of the transition state method to the calculation of reaction velocities, especially in solution Trans. Faraday Soc. 31:875–894.
5. Rice O. K, Ramsperger H. C. (1928) Theories of unimolecular gas reactions at low pressures. II J. Am. Chem. Soc. 50:617–620.
6. Kassel L. S. (1928) Studies in homogeneous gas reactions. II. introduction of quantum theory J. Phys. Chem. 32:1065–1079.
7. Marcus R. A. (1952) Unimolecular dissociations and free radical recombination reactions J. Chem. Phys. 20:359–364.
8. Keck J. C. (1967) Variational theory of reaction rates Adv. Chem. Phys. 13:85–121.
9. Truhlar D. G, Garrett B. C. (1980) Variational transition-state theory Acc. Chem. Res. 13:440–448.
10. Uzer T, Jaffé C, Palacián J, Yanguas P, Wiggins S. (2002) The geometry of reaction dynamics Nonlinearity 15:957–992.
11. Komatsuzaki T, Berry R. S. (1999) Regularity in chaotic reaction paths. I. Ar_6 J. Chem. Phys. 110:9160–9173.
12. Jaffe C, Ross S. D, Lo M. W, Marsden J, Farrelly D, Uzer T. (2002) Statistical theory of asteroid escape rates Phys. Rev. Lett. 89:011101_1–011101_4.
13. Karplus M. (2000) Aspects of protein reaction dynamics: Deviations from simple behavior J. Phys. Chem. B 104:11–27.
14. Lovejoy E. R, Kim S. K, Moore C. B. (1992) Observation of Transition-State Vibrational Thresholds in the Rate of Dissociation of Ketene Science 256:1541-1544; Lovejoy E. R, Moore C. B. (1993) Structures in the energy dependence of the rate constant for ketene isomerization J. Chem. Phys. 98:7846-7854.
15. Miller W. H. (1977) Semi-classical theory for non-separable systems:. construction of good action-angle variables for reaction rate constants Faraday Discussions Chem. Soc. 62:40–46.
16. Marcus R. A. (1992) Skiing the reaction rate slopes Science 256:1523–1524.
17. Hernandez R, Miller W. H. (1993) Semiclassical transition state theory. a new perspective Chem. Phys. Lett. 214:129–136.
18. Amitrano C, Berry R. S. (1992) Probability distributions of local liapunov exponents for small clusters Phys. Rev. Lett. 68:729–732.
19. Hinde R. J, Berry R. S. (1993) Chaotic dynamics in small inert gas clusters: The influence of potential energy saddles J. Chem. Phys. 99:2942–2963.
20. Komatsuzaki T, Berry R. S. (2001) Proc. Nat. Acad. Sci. USA 98:7666.
21. Komatsuzaki T, Berry R. S. (2002) Chemical reaction dynamics: Many-body chaos and regularity Adv. Chem. Phys. 123:79.
22. Toda M, Komatsuzaki T, Konishi T, Berry R. S, Rice S. A, eds. (2005) Geometrical Structures of Phase Space in Multidimensional Chaos: Applications to Chemical Reaction Dynamics in Complex Systems, Adv. Chem. Phys. Vol. 130A,130B. and references therein.
23. Kramers H. A. (1940) Brownian motion in a field of force and the diffusion model of chemical reactions Physica 7:284–304.
24. Grote R. F, Hynes J. T. (1980) The stable states picture of chemical reactions. II. rate constants for condensed and gas phase reaction models J. Chem. Phys. 73:2715–2732.
25. Mori H. (1965) Transport, collective motion, and brownian motion Prog. Theor. Phys. 33:423–455.
26. Zwanzig R. (1973) Nonlinear generalized langevin equations J. Stat. Phys. 9:215–220.
27. van der Zwan G, Hynes J. T. (1983) Nonequilibrium solvation dynamics in solution reactions J. Chem. Phys. 78:4174–4185.
28. Tokuyama M, Mori H. (1976) Statistical-mechanical theory of random frequency modulations and generalized browninan motion Prog. Theor. Phys. 55:411–429.
29. Nitzan A, Ortoleva P, Deutch J, Ross J. (1974) Fluctuations and transitions at chemical instabilities: The analogy to phase transitions J. Chem. Phys. 61:1056–1074.
30. Berezhkovskii A. M, Pollak E, Zitserman V. Y. (1992) Activated rate processes: Generalization of the kramers-grote-hynes and langer theories J. Chem. Phys. 97:2422–2437.
31. Pollak E, Talkner P. (1993) Activated rate processes: Finite-barrier expansion for the rate in the spatial-diffusion limit Phys. Rev. E 47:922–933.
32. Pollak E, Berezhkovskii A. M, Schuss Z. (1994) Activated rate processes: A realation between hamiltonian and stochastic theories J. Chem. Phys. 100:334–339.
33. Ryter E. (1987) Noise-induced transitions in a double-well potential at low friction J. Stat. Phys. 49:751–765.
34. Klosek M. M, Matkowsky B. J, Schuss Z. (1991) The kramers problem in the turnover regime: The role of the stochastic separatirx Ber. Bunsenges. Phys. Chem. 95:331–337.
35. Martens C. C. (2002) Qualitative dynamics of generalized langevin equations and the theory of chemical reaction rates J. Chem. Phys. 116:2516–2528.
36. Müller K, Brown L. D. (1979) Location of saddle points and minimum energy paths by a constrained simplex optimization procedure Theor. Chim. Acta 53:75–93.
37. Ermak D. L, Buckholz H. (1980) Numerical integration of the langevin equation: Monte carlo simulation J. Comp. Phys. 35:169–182.
38. Bartsch T, Hernandez R, Uzer T. (2005) Transition state in a noisy environment Phys. Rev. Lett. 95:058301_1–058301_4.
39. Bartsch T, Uzer T, Hernandez R. (2005) Stochastic transition states: Reaction geometry amidst noise J. Chem. Phys. 123:204102_1–204102_14.
40. Bartsch T, Uzer T, Moix J. M, Hernandez R. (2006) Identifying reactive trajectories using a moving transition state J. Chem. Phys. 124:244310_1–244310_13.
41. Bartsch T, Moix J. M, Hernandez R, Kawai S, Uzer T. (2008) Time-dependent transition state theory Adv. Chem. Phys. 140:191–238.
42. Kawai S, Bandrauk A. D, Jaffé C, Bartsch T, Palacián J, Uzer T. (2007) Transition state theory for laser-driven reactions J. Chem. Phys. 126:164306_1–164306_12.
43. Polanyi J. C, Zewail A. H. (1995) Direct observation of the transition state Acc. Chem. Res 28:119–132.
44. Waalkins H, Schubert R, Wiggins S. (2008) Wigner's dynamical transition state theory in phase space: classical and quantum Nonlinearity 21:R1–R118.
45. Schuch D. (1999) Effective description of the dissipative interaction between simple mode-systems and their environment Int. J. Quant. Chem. 72:537–547.
46. Leung A. Y. T, Zhang Q. C. (2003) Normal form computation without central manifold reduction J. Sound Vib. 266:261–279.
47. Deprit A. (1969) Canonical transformations depending on a small parameter Cel. Mech. 1:12.